Journal of Analytical Science & Technology (2011) 2 (Suppl A), A8-A14
Proceeding www.jastmag.org
DOI 10.5355/JAST.2011.A8

Plenary Lecture Ⅱ **Open Access**

The Nature of Magnetic State of Small Fe_3O_4 Nanoparticles

U. Sobočan[1], Gaehang Lee[2], Hyun-Wook Kang[3], Hae Jin Kim[2,3,*], Z. Jagličić[4], J. Dolinšek[1,5,*]

[1]J. Stefan Institute & University of Ljubljana, Faculty of Mathematics and Physics, Jamova 39, SI-1000 Ljubljana, Slovenia
[2]Division of Materials Science, Korea Basic Science Institute, Daejeon 305–806, Republic of Korea
[3]Graduate School of Analytical Science and Technology, Chungnam National University, Daejeon 305-764, Republic of Korea
[4]Institute of Mathematics, Physics and Mechanics & University of Ljubljana, Faculty of Civil and Geodetic Engineering, Jamova 2, SI-1000 Ljubljana, Slovenia
[5]EN–FIST Centre of Excellence, Dunajska 156, SI-1000 Ljubljana, Slovenia

***Corresponding author:**
Hae Jin Kim, E-mail: hansol@kbsi.re.kr
J. Dolinšek, E-mail: jani.dolinsek@ijs.si

From 2011 International Symposium on Analytical Science and Technology (ISAST)
Daejeon, Chungnam, Republic of Korea, 15-17 November, 2011

Abstract

We have investigated the nature of the magnetic state of 4 nm and 7 nm magnetite Fe_3O_4 nanoparticles and show that they form a collective superspin glass state. Magnetic force on the nanoparticles relevant to the tumor targeting application was determined as well.

Key words: magnetite Fe_3O_4; nanoparticles; magnetic properties; superspin glass

Introduction

Magnetic nanoparticles are attractive systems for a wide range of applications in science, technology and medicine, such as data storage, MRI contrast agents, medical drug delivery and hyperthermia [1,2]. The magnetite (Fe_3O_4) nanoparticles with diameters d less than 20 nm and a narrow size distribution are of special importance to the development of high-performance magnetoelectronic nanodevices and biomedical materials due to the high magnetic dipole moment of the

nanoparticles and biocompatibility. While the magnetite nanoparticles of diameters larger than 20 nm are ferrimagnetic (in accordance with the bulk Fe_3O_4 that is ferrimagnetic below 858 K), the particles gradually become superparamagnetic when their size decreases below that value. The magnetic behavior of a system of Fe_3O_4 nanoparticles depends on the coupling between their magnetic moments [3–5]. Very small nanoparticles (d < 5 nm) are considered to interact only weakly, so that their magnetic state can be well approximated by a superparamagnetic (SP) state of independent giant magnetic moments up to several hundred Bohr magnetons μ_B, whereas larger nanoparticles interact strongly to produce a collective "superspin" glass state (SSG). In this paper, we examine the magnetic behavior of small Fe_3O_4 nanoparticles of diameters d = 4 and 7 nm and show that the genuine SP limit of independent moments is not reached even for the smaller size (4 nm).

Results and Discussion

The Fe_3O_4 nanoparticles were synthesized from commercial Iron(III) acetylacetonate (97%, Aldrich), 1-hexadecanol (95%, Aldrich), toluene (99%, Junsei), and ethanol (99%, Junsei), without further purification. Fe(acetylacetonate: acac)$_3$ (2 g) and 1-hexadecanol (10 mL) were mixed in a 100 mL two-necked round-bottom flask with stirring at 50°C under air atmosphere for 1 h. To synthesize the 4 nm (or 7 nm) Fe_3O_4 nanoparticles, the reaction mixture was heated up to 260°C (or 330°C) for 30 min and allowed for 2 h to yield a black-brown dispersion. The mixture was cooled to room temperature and the product was precipitated by adding ethanol (30 mL). Centrifugation at 4,000 rpm and repeated washing with ethanol and toluene for 10 min were performed to yield Fe_3O_4 nanoparticles. The obtained particles could be readily dispersed in various hydrocarbon solvents such as toluene, hexane, and chlorobenzene.

The nanoparticles were characterized by TEM imaging using Omega EM912 microscope operated at 120 kV and X-ray diffraction using Bruker D8 advance diffractometer with a monochromatized Cu-Kα radiation at 40 kV and 40 mA. The TEM images showed that the Fe_3O_4 nanoparticles display high monodispersity in size of d = 4.1 ± 0.3 nm (Fig. 1a) and d = 7.2 ± 0.6 nm (Fig. 1b). In the following, these nanoparticles will be denoted shortly as the 4 nm and 7 nm particles.

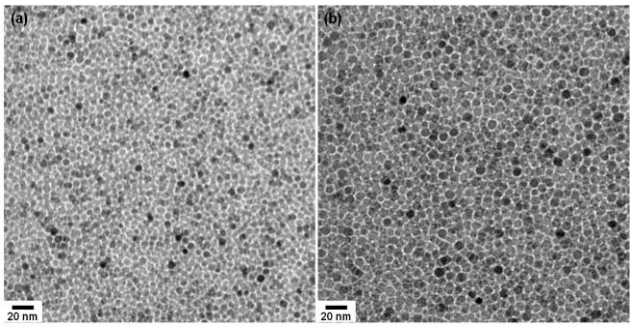

Fig. 1. TEM images of (a) 4.1 ± 0.3 nm Fe_3O_4 and (b) 7.2 ± 0.6 nm Fe_3O_4 nanoparticles.

The X-ray patterns (Fig. 2) show good crystallinity for both nanoparticle sizes, as evidenced by comparing to the stick spectra of bulk magnetite. Magnetic measurements were conducted using a QD MPMS XL-5 SQUID magnetometer equipped with a 50 kOe magnet and operating in the temperature range between 1.9 and 400 K.

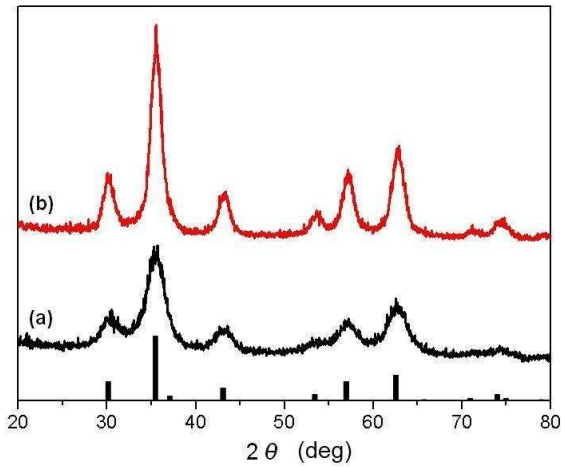

Fig. 2. XRD patterns of (a) 4.1 ± 0.3 nm Fe_3O_4 and (b) 7.2 ± 0.6 nm Fe_3O_4 nanoparticles. The standard peaks of bulk magnetite from the JCPDS card No. 19-0629 are shown as a bar diagram at the bottom.

Our magnetic experiments started with the determination of the magnetization versus the magnetic field curves, $M(H)$, in the field range ± 50 kOe at the temperature T = 300 K (Fig. 3). At such high temperature, the $M(H)$ data can be well described by the expression

$$M = M_0 L(\mu H / k_B T), \qquad (1)$$

where M_0 is the saturation magnetization, $L(y) = \coth(y) - 1/y$ is the Langevin function, and $\mu = x\mu_B$ is the magnetic moment (the "superspin") of the nanoparticle. The fits (solid curves in Fig. 3) yielded the M_0 and x values that are collected in Table 1.

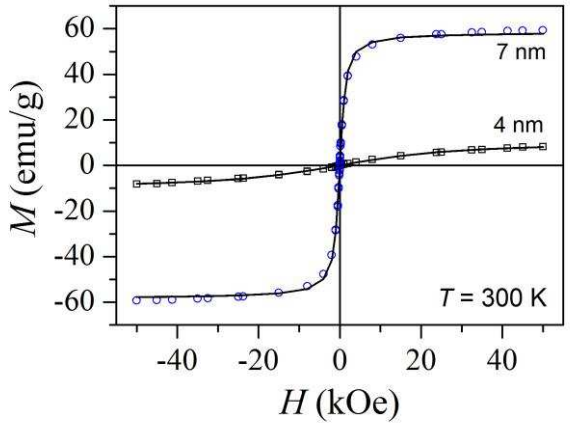

Fig. 3. Magnetization versus the magnetic field, M(H), curves at T = 300 K of the 4 nm and 7 nm Fe_3O_4 nanoparticles. Solid curves are fits with Eq. (1).

Table 1. Parameters M_0, x and the particles' diameters determined from the $M(H)$ fits.

d / nm (from TEM)	M_0 / emu/g	x	d / nm (from $M(H)$)
4.1 ± 0.3	10.1 ± 0.5	424 ± 21	4.9 ± 0.3
7.2 ± 0.6	58.4 ± 0.3	7648 ± 166	7.6 ± 0.4

The 4 nm particles possess a superspin μ = 424 μ_B, whereas the superspin of the 7 nm particles is μ = 7648 μ_B. The M_0 and x values can be used for an independent evaluation of the particles' diameters by writing

$$\mu = x\mu_B = M_0 \rho V \ , \qquad (2)$$

where ρ is the Fe_3O_4 density (amounting 5.21 g/cm^3) and V is the nanoparticle volume. Considering spherical shape of the nanoparticles, we obtain the diameter values d = 4.3 ± 0.3 nm and d = 7.6 ± 0.4 nm that match well the values obtained from the TEM images.

Knowing the superspin values, we are able to estimate the magnetic dipole-dipole interaction between two neighboring nanoparticles that plays a role in the anisotropy energy of a magnetic moment. Assuming that the particles are touching, the strength of this interaction can be evaluated from the expression

$$E_{d-d} = (\mu_0 / 4\pi)\mu^2 / d^3 \ , \qquad (3)$$

yielding an estimate (in temperature units) E_{d-d}^{4nm} =1.6 K and E_{d-d}^{7nm} =97 K. The dipole-dipole interaction is thus quite strong for the 7 nm particles, whereas it is considerably weaker for the 4 nm particles.

The SP and the SSG states both show very similar spin freezing dynamics below the freezing (or blocking) temperature T_f , resulting in broken-ergodicity phenomena like the difference between the field-cooled (fc) and the zero-field-cooled (zfc) magnetic susceptibilities below T_f in small magnetic fields, the frequency-dependent cusp in the zfc susceptibility, associated with a frequency-dependent freezing temperature, $T_f(\nu)$, and slow relaxation effects in the dc magnetization below T_f with time constants longer than any experimentally accessible time scale. The SP and the SSG states can be experimentally discriminated by three criteria:

(1) the temperature dependence of the fc susceptibility below T_f , which is flat (constant) in SSGs due to ultrametric organization of the free-energy phase space [6], whereas it continues to grow down to the lowest temperature in the SP state of noninteracting spins due to validity of the Curie law, $\chi_{fc} = N\mu^2 / 3k_B T$ (where N is the superspin density);

(2) the magnitude of the the relative shift of $T_f(\nu)$ per decade of frequency, expressed by the empirical criterion $\Gamma = \Delta T_f / T_f \Delta(\log \nu)$. Spin glasses are characterized by values Γ <0.06, whereas $\Gamma \approx$ 0.3 in SPs [7];

(3) the existence of memory effect (ME) in a zfc experiment, where the cooling history of the sample in zero field involving isothermal aging time intervals can be retrieved upon measuring the zfc magnetization in a subsequent heating run. While the ME is present in the collective SSG state, it is absent

in the SP state of noninteracting spins [8–11].

In the following we present the measurements of the zfc and fc dc susceptibility, the ac susceptibility and the ME on the 4 nm and 7 nm Fe_3O_4 nanoparticles and discuss the results in view of the above three criteria, in order to find out whether the investigated nanoparticles can be classified as SPs or SSGs.

The zfc and fc dc susceptibilities $\chi = M/H$ were determined in the temperature range 1.9 – 300 K in the magnetic field H = 100 Oe. For the 4 nm nanoparticles (Fig. 4a), χ_{zfc} exhibits a maximum at the freezing (blocking) temperature T_f = 19.2 K, whereas χ_{fc} continues to grow strongly below T_f with a tendency that the growth becomes weaker upon approaching the $T \rightarrow 0$ limit. The 7 nm nanoparticles (Fig. 4b) exhibit the maximum in χ_{zfc} at $T_f = 107$ K, whereas the growth of χ_{fc} below T_f is very weak with a tendency to saturate to a constant plateau.

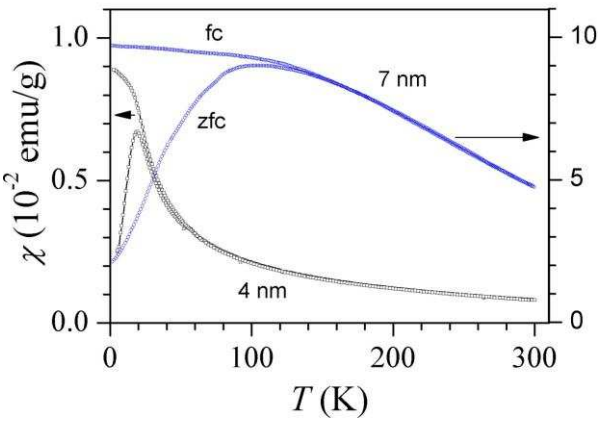

Fig. 4. The zfc and fc dc magnetic susceptibilities $\chi = M/H$ of 4 nm and 7 nm Fe_3O_4 nanoparticles in the temperature range 1.9 – 300 K in a magnetic field H = 100 Oe.

The significantly higher T_f of the 7 nm nanoparticles is compatible with their larger magnetic moments and higher anisotropy energy, which causes the superspin reorientations to freeze at a higher temperature. The almost constant χ_{fc} below T_f of the 7 nm nanoparticles reveals strong interactions between the superspins and the collective SSG state. The estimated dipolar anisotropy E_{d-d}^{7nm} =97 K is in qualitative agreement with the T_f = 107 K value of the 7 nm nanoparticles and is very likely the dominant source of the superspin coupling that leads to the SSG state. In contrast, the strongly growing χ_{fc} of the 4 nm nanoparticles below T_f upon cooling suggests their SP nature. However, weak dipolar interactions between the superspins may still be present (recall that the dipolar coupling between the 4 nm nanoparticles has been estimated to E_{d-d}^{4nm} =1.6 K), though they cannot be confirmed from the temperature-dependence of the fc susceptibility below T_f. The weaker growth of the fc susceptibility in the $T \rightarrow 0$ limit can either originate from the blocking effect in the absence of interactions [11] or from weak interspin interactions, so that the fc susceptibility cannot discriminate between the weakly coupled and uncoupled superspins in this case. The zfc and fc susceptibility experiments thus reveal that the 7 nm nanoparticles create a collective SSG state below the freezing temperature T_f = 107 K, whereas the 4 nm nanoparticles form a spin-blocked state below T_f = 19.2 K that is SP-like, but weak interspin interactions cannot be excluded.

The ac susceptibility was measured in an ac magnetic field of amplitude H_0 = 6.5 Oe at the frequencies ν = 1, 10, 100 and 1000 Hz. The real part of the susceptibility χ' of the 4 nm nanoparticles is displayed in Fig. 5a.

χ' exhibits a frequency-dependent cusp at a temperature that we associate with the frequency-dependent freezing temperature $T_f(\nu)$. At ν = 1 Hz the cusp occurs at 23.1 K, whereas it is shifted to 25.4 K at ν = 1 kHz (inset in Fig. 5a). The relative shift of $T_f(\nu)$ per decade of frequency amounts Γ = 0.03, which is in the range characteristic of spin glasses like <u>*Au*</u>Fe and <u>*Pd*</u>Mn [7] (for superparamagnets, Γ is one order of magnitude larger). The χ' susceptibility of the 7 nm nanoparticles is displayed in Fig. 5b. At ν = 1 Hz the cusp in χ' occurs at 136 K, whereas it is shifted to 150 K at ν = 1 kHz (inset in Fig. 5b), yielding the same value Γ = 0.03. According to the relative shift of $T_f(\nu)$ per decade of frequency criterion, the 4 nm and 7 nm nanoparticles both classify as SSGs.

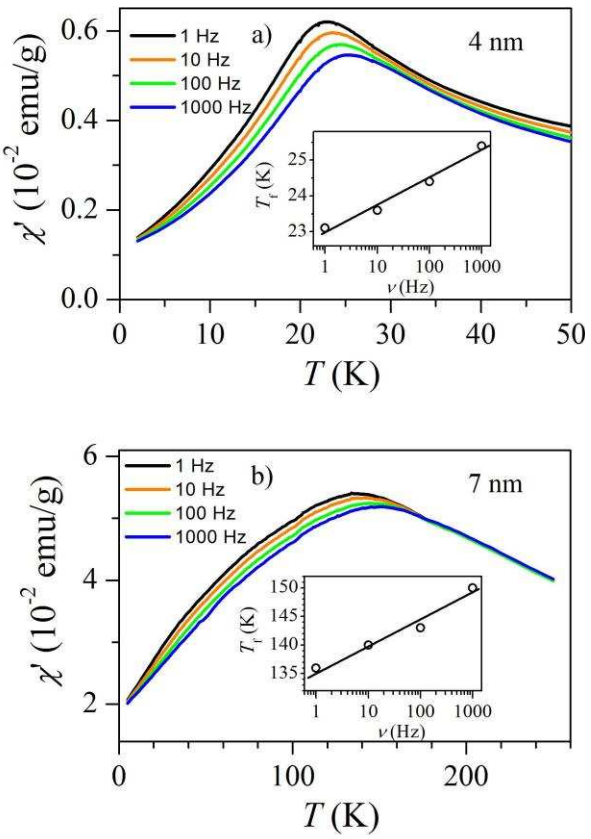

Fig. 5. Real part χ' of the ac susceptibility of (a) 4 nm and (b) 7 nm Fe_3O_4 nanoparticles. The frequency-dependent temperature T_f of the maximum in χ' is shown in the insets.

The ME is the most spectacular manifestation of the out-of-equilibrium dynamics of a nonergodic system of coupled spins in a frustrated configuration, where the spin state reached at a given temperature upon isothermal aging for a time t_w can be retrieved after a negative temperature cycle. In a genuine zfc ME experiment, the spin system is cooled continuously in zero magnetic field from the paraphase through the freezing temperature T_f to the nonergodic phase and the cooling is stopped at $T_1 < T_f$ for a time t_w of the order of minutes to hours. The cooling then resumes to the lowest temperature, where a small magnetic field is applied and the zfc magnetization is measured in a continuous heating run. The memory is imprinted in the zfc magnetization M_{zfc}, which shows a dip (a diminution) at the temperature T_1 of aging. The physics of the ME is still incompletely understood. According to the spin-droplet theory [12,13], quasiequilibrated spin domains are formed within the spin-glass matrix during the aging period t_w, which can be destroyed by the thermal energy upon heating at a slightly higher temperature than where they were formed. The ME is present only in systems of coupled spins in a frustrated configuration like spin glasses, whereas it is absent in systems of noninteracting spins like SPs. Here it is worth mentioning an interesting recent technological application of the ME, which provides basis of the thermal storage of digital information, where the digital data are stored into a thermal memory cell by pure thermal manipulation in the absence of an electric or magnetic field [14].

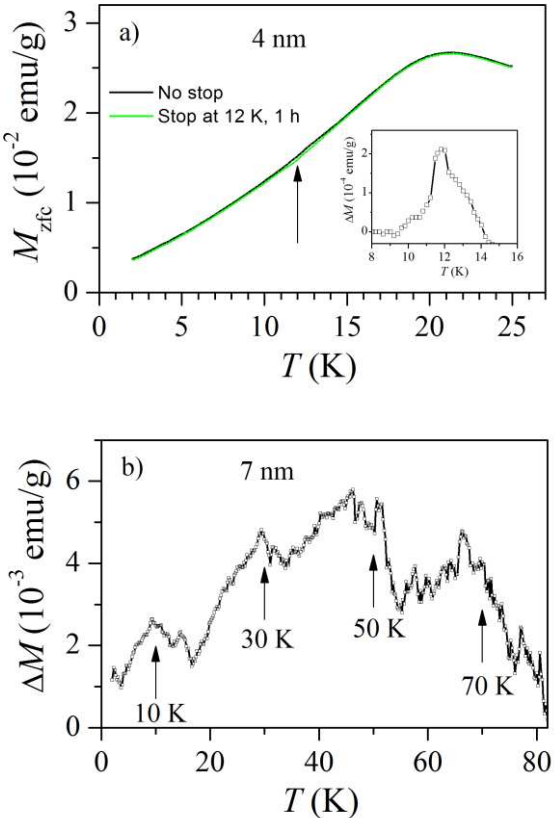

Fig. 6. (a) ME in the system of 4 nm Fe_3O_4 nanoparticles for the stop temperature T_1 = 12 K and aging time t_w = 1 h. $M_{zfc}(t_w)$ shows a diminution at T_1 (marked by an arrow) with respect to the reference (unaged) curve $M_{zfc}(0)$. The difference $\Delta M = M_{zfc}(0) - M_{zfc}(t_w)$ is shown in the inset. (b) ME in the system of 7 nm nanoparticles. The difference plot ΔM is shown for four consecutive stops at T_1 = 70, 50, 30 and 10 K (marked by arrows) by aging for t_w = 1 h at each stop temperature.

The ME experiment on the 4 nm nanoparticles was performed by cooling in zero field through $T_f = 19.2$ K with a rate of 2 K/min to the temperature T_1 = 12 K, where the cooling was temporarily stopped and the spin system was let to age there isothermally for a time t_w = 1 h.

After aging, the cooling resumed to 2 K. At the lowest temperature, a small magnetic field H = 4 Oe was applied and M_{zfc} was measured in a heating run with the rate of 0.3 K/min to a temperature above T_f. A reference run with no stop (t_w = 0) at T_1 was also performed. The ME is manifested as a drop of M_{zfc} in the vicinity of T_1 = 12 K of the aged curve with respect to the reference (unaged) curve $M_{zfc}(t_w = 0)$ (Fig. 6a). The difference $\Delta M = M_{zfc}(0) - M_{zfc}(t_w)$ is shown in the inset of Fig. 6a, exhibiting a peak at the aging temperature T_1. The presence of the ME in the system of 4 nm nanoparticles is convincing evidence that the Fe_3O_4 superspins are coupled and form a collective SSG state below T_f.

The ME experiment on the 7 nm nanoparticles was conducted by cooling in zero field through the freezing temperature into the nonergodic phase and then performing four consecutive stops for t_w = 1 h at the temperatures T_1 = 70, 50, 30 and 10 K. A reference run with no stop was performed as well. The difference plot $\Delta M = M_{zfc}(0) - M_{zfc}(t_w)$ is shown in Fig. 6b. The four peaks in ΔM at the selected stop temperatures demonstrate that all four stops during zfc cooling have been memorized by the superspin system, confirming that the 7 nm nanoparticles are magnetically coupled and form a SSG state.

The above experimental results confirm that the systems of 4 nm and 7 nm Fe_3O_4 nanoparticles both belong to the SSG class of coupled superspins and the true SP limit of uncoupled spins is not reached even for the smaller (4 nm) nanoparticles. However, in the room-temperature applications, such as MRI contrast agents, medical drug delivery and hyperthermia, thermal reorientations of the superspins are fast enough to overwhelm the interspin interactions and the superspins of both the 4 nm and the 7 nm Fe_3O_4 nanoparticles behave as a system of independent superparamagnetic spins. In this context, an interesting application of targeting cancerous tumors with liposome cans containing embedded Fe_3O_4 nanoparticle clusters that can be moved *in situ* under the influence of an external magnet was reported recently [15]. The methodology presented in our paper allows determining the magnetic force on an individual Fe_3O_4 nanoparticle by knowing the magnetic field data of the applied magnet used to drag the nanoparticles. A typical magnet for such application is e.g. a disk-shaped cylindrical Nd-Fe-B permanent magnet of diameter 10 mm and thickness 2 mm. The magnetic field density on the disk axis (assuming to point along the z direction of a coordinate system) at the magnet surface is typically B = 400 mT, whereas the magnetic field gradient is $\partial B/\partial z$ = 38 T/m. The maximum magnetic force on a nanoparticle with the superspin μ , assumed to be located at the magnet surface on the axis is

$$F = \mu \partial B/\partial z \,. \qquad (4)$$

The force on a single Fe_3O_4 nanoparticle of 4 nm diameter with the superspin value given in Table 1 amounts $F^{4nm} = 1.5\times10^{-19}$ N, whereas the force on a 7 nm nanoparticle is one order of magnitude larger, amounting $F^{7nm} = 2.7\times10^{-18}$ N. Magnetic force on a cluster containing n_0 nanoparticles is, of course, n_0- times larger. A comparison to the gravitational force acting on a single nanoparticle in the Earth's gravity field (calculated from $F_g = (\pi/6)\rho d^3 g$, where g = 9.81 ms^{-2} is the gravitational acceleration) shows that the magnetic force exceeds the gravitational force by two orders of magnitude, (i.e., $F^{4nm}/F_g^{4nm} \approx 100$ and $F^{7nm}/F_g^{7nm} \approx 300$), so that dragging the Fe_3O_4 nanoparticles by an external magnet in the tumor targeting application is promissing. In comparison, the magnetic moment of the maghemite Fe_2O_3 nanoparticles is considerably smaller, so that those nanoparticles are less appropriate for the magnetic targeting.

References

1. Dormann, J.L.; Tronc, E.; and Fiorani, D. Magnetic relaxation in fine-particle systems. *Adv. Chem. Phys.* **1997**, *98*, 283-494.
2. Himpsel, F.J.; Ortega, J.E.; Mankey, G.J.; and Willis, R.F. Magnetic nanostructures. *Adv. Phys*. **1998**, *47*, 511-597.
3. Suzuki, M.; Fullem, S.I.; Suzuki, I.S.; Wang, L.; and Zhong,

C.-J. Observation of superspin-glass behavior in Fe_3O_4 nanoparticles. *Phys. Rev.* B **2009**, *79*, 024418.

4. Goya, G.F.; and Morales, M.P. Field dependence of blocking temperature in magnetite nanoparticles. *J. Metastable and Nanocryst. Mater.* **2004**, *20-21*, 673-678.
5. Hayashi, K.; Sakamoto, W.; and Yogo, T. Magnetic and rheological properties of monodisperse Fe_3O_4 nanoparticle/organic hybrid. *J. Magn. Magn. Mater.* **2009**, *321*, 450-457.
6. Binder, K.; and Young, A.P. Spin glasses: Experimental facts, theoretical concepts, and open quastions. *Rev. Mod. Phys.* **1986**, *58*, 801-976.
7. Mydosh, J. A. *Spin glasses: An Experimental Introduction*; Taylor & Francis: London, 1993; p67.
8. Sahoo, S.; Petracic, O.; Kleemann, W.; Nordblad, P.; Cardoso, S.; and Freitas, P.P. Aging and memory in a superspin glass. *Phys. Rev.* B **2003**, *67*, 214422.
9. Sun, Y.; Salamon, M.B.; Garnier, K.; and Averback, R.S. Memory effects in an interacting magnetic nanoparticle system. *Phys. Rev. Lett.* **2003**, *91*, 167206.
10. Cador, O.; Grasset, F.; Haneda, H.; and Etourneau, J. Memory effect and super-spin-glass ordering in an aggregated nanoparticle sample. *J. Magn. Magn. Mater*. **2004**, *268*, 232-236.
11. Sasaki, M.; Jönsson, P.E., Takayama, H.; and Mamiya, H. Aging and memory effects in superparamagnets and superspin glasses. *Phys. Rev.* B **2005**, *71*, 104405.
12. Fisher, D.S.; and Huse, D.A. Nonequilibrium dynamics of spin glasses. *Phys. Rev.* B **1988**, *38*, 373-385.
13. Fisher, D.S.; and Huse, D.A. Equilibrium behavior of the spin-glass ordered phase. *Phys. Rev.* B **1988**, *38*, 386-411.
14. Dolinšek, J.; Feuerbacher, M.; Jagodič, M.; Jagličić, Z.; Heggen, M.; and Urban, K. A thermal memory cell. *J. Appl. Phys*. **2009**, *106*, 043917.
15. Mikhaylov, G.; *et al*. (15 authors), Ferri-liposomes as an MRI-visible drug-delivery system for targeting tumors and their microenvironment. *Nature Nanotechnology* **2011**, *6*, 594-602.